Phytochemistry 111 (2015) 72–83

Contents lists available at ScienceDirect

Phytochemistry

journal homepage: www.elsevier.com/locate/phytochem

Fruits from ripening impaired, chlorophyll degraded and jasmonate insensitive tomato mutants have altered tocopherol content and composition

Juliana Almeida [a], Ramón Asís [b], Virginia Noel Molineri [b], Ivan Sestari [c], Bruno Silvestre Lira [a], Fernando Carrari [d], Lázaro Eustáquio Pereira Peres [e], Magdalena Rossi [a,*]

[a] Departamento de Botânica, Instituto de Biociências, Universidade de São Paulo, São Paulo, SP, Brazil
[b] CIBICI, Facultad de Ciencias Químicas, Universidad Nacional de Córdoba, Córdoba, Argentina
[c] Universidade Federal de Santa Catarina, Campus Curitibanos, Curitibanos, SC, Brazil
[d] Instituto de Biotecnología, Instituto Nacional de Tecnología Agropecuaria and Consejo Nacional de Investigaciones Científicas y Técnicas, Hurlingham, Buenos Aires, Argentina
[e] Departamento de Ciências Biológicas, Escola Superior de Agricultura "Luiz de Queiroz", Universidade de São Paulo, Piracicaba, SP, Brazil

ARTICLE INFO

Article history:
Received 2 August 2014
Received in revised form 20 October 2014
Available online 25 November 2014

Keywords:
Tomato mutants
Solanum lycopersicum
Solanaceae
Atocopherol
Carotenoids
Chlorophyll
Jasmonic acid
Ripening
Antioxidant capacity

ABSTRACT

Since isoprenoids are precursors in chlorophyll, carotenoid and tocopherol pathways, the study of their metabolism is of fundamental importance in understanding the regulatory cross-talk that contributes to the nutritional quality of tomato fruits. By means of an integrated analysis of metabolite and gene expression profiles, isoprenoid metabolism was dissected in ripening-impaired (*ripening inhibitor* and *non-ripening*), senescence-related (*lutescent1* and *green flesh*) and jasmonate insensitive (*jasmonic acid insensitive 1-1*) tomato mutants, all in the Micro-Tom genetic background. It was found that the more upstream the location of the mutated gene, the more extensive the effect on the transcriptional profiles of the isoprenoid-related genes. Although there was a distinct effect in the analyzed mutations on chlorophyll, carotenoid and tocopherol metabolism, a metabolic adjustment was apparent such the antioxidant capacity mostly remained constant. Transcriptional profiles from fruits of ripening and senescence-related tomato mutants suggested that maintenance of the *de novo* phytyl diphosphate synthesis might, in later ripening stages, compensate for the lack of chlorophyll-derived phytol used in tocopherol production. Interestingly, an impairment in jasmonate perception led to higher total tocopherol levels in ripe fruits, accompanied by an increase in antioxidant capacity, highlighting the contribution of tocopherols to this nutritionally important trait.

1. Introduction

Fruit ripening involves a series of coordinated biochemical and physiological processes resulting in organoleptic changes in texture, aroma and color (Seymour et al., 1993). One of the most important and visible changes in tomato (*Solanum lycopersicum* L.), a climacteric fruit, involves de-greening and accumulation of carotenoids; a phenomenon that is associated with a chloroplast-to-chromoplast transition (Egea et al., 2011). Tomato is one of the most consumed fruits worldwide and is a major source of many dietary nutrients, such as minerals, antioxidants and vitamins; all of which contribute to the prevention of chronic diseases (Seybold et al., 2004; Perez-Fons et al., 2014). In particular tocopherols, which belong to the vitamin E (VTE) family, are potent lipid soluble antioxidant molecules that reduce free-radical damage to membrane lipids by scavenging peroxyl radicals (Brigelius-Flohé et al., 2002; Niki and Traber, 2012). Tocopherols can also act as scavengers of singlet oxygen ($^1O_2$) and, in plants, this function is related to protection of the photosynthetic apparatus from oxygen toxicity (Trebst, 2003; Krieger-Liszkay and Trebst, 2006).

Tocopherols are isoprenoid-derived compounds that are synthesized from the condensation of a chromanol ring and a prenyl side-chain from the shikimate (SK) and 2-C-methyl-D-erythritol 4-phosphate (MEP) pathways, respectively (Dellapenna and

* Corresponding author at: Departamento de Botânica, Instituto de Biociências, Universidade de São Paulo, Rua do Matão, 277, 05508-900 São Paulo, Brasil. Tel.: +55 11 3091 7556; fax: +55 11 3091 7547.
E-mail addresses: juliana.almeida.silva@usp.br (J. Almeida), rasis@fcq.unc.edu.ar (R. Asís), vicky_412@hotmail.com (V.N. Molineri), ivan.sestari@ufsc.br (I. Sestari), bslira.bsl@gmail.com (B.S. Lira), carrari.fernando@inta.gob.ar (F. Carrari), lazaro.peres@usp.br (L.E.P. Peres), mmrossi@usp.br (M. Rossi).

http://dx.doi.org/10.1016/j.phytochem.2014.11.007
0031-9422/

Pogson, 2006). The MEP pathway also provides precursors for other plastid isoprenoids, such as chlorophylls (Chls) and carotenoids, the latter of which can be divided into two classes based on their chemical structures: linear or cyclized hydrocarbons, termed carotenes, and xanthophylls that are oxygenated derivatives of carotenes. The xanthophylls lutein, violaxanthin and neoxanthin are components of the light harvesting complex (LHC) and act both as antenna pigments and as protective molecules, by reducing the production of reactive oxygen species (ROS). β-Carotene is a component of the photosynthetic reaction center (Dall'Osto et al., 2006) and during tomato fruit ripening, it accumulates together with the primary ripening-related pigment lycopene (Bramley, 2002).

A recent study focusing on the transcriptional regulation of tocopherol biosynthesis in tomato (cv. M82) (Quadrana et al., 2013) showed that expression of genes encoding enzymes of the tocopherol-core, MEP and SK pathways are controlled both temporally and spatially, and that the supply of the prenyl donor, phytyl diphosphate, appears to be a limiting step in VTE accumulation at later fruit stages. In *Arabidopsis thaliana*, it has been shown that phytyl diphosphate for tocopherol biosynthesis can also originate from the activity of phytol kinase (VTE5), which functions in phytol recycling after Chl degradation (Ischebeck et al., 2006; Valentin et al., 2006). The strong correlation between the expression of *VTE5* and the VTE biosynthetic genes, and the content of Chls and VTE in tomato leaves and fruits supports the contribution of phytol recycling enzymes to tocopherol biosynthesis in this species as well (Quadrana et al., 2013).

This metabolic cross-talk suggests that changes in carotenoid biosynthesis and Chl metabolism might affect tocopherol content, but a better understanding of the accumulation of these metabolites depends on deciphering the complexity of the isoprenoid metabolic network and its branching (Vranová et al., 2012). To this end, senescence and ripening-related tomato mutants represent potentially excellent models, since they provide a means to study metabolic fluxes between these pathways (Table 1). *Non-ripening* (*nor*) and *ripening inhibitor* (*rin*) are tomato mutants with impaired fruit ripening, which fail to undergo typical ripening-related *de novo* carotenoid biosynthesis and Chl degradation (Giovannoni, 2004). Another mutant, *green flesh* (*gf*) is deficient in the STAY-GREEN1 (SGR1) protein involved in destabilization of the Chl-apoprotein complexes and recruitment of the Chl catabolic enzymes, which are a prerequisite for Chl catabolism; thus the fruit retains Chls even at the ripe stage (Barry et al., 2008; Park et al., 2007; Hörtensteiner, 2009). In contrast, the *lutescent* (*l*) mutant displays premature leaf senescence and its fruits lack Chl (Barry et al., 2012).

The ethylene and cytokinin signaling pathways are well-defined and mediate senescence and de-greening, while other hormones, such as jasmonic acid (JA), have also been demonstrated to affect these processes (Lim et al., 2007). Altered patterns of senescence and de-greening have been reported in JA-insensitive or JA-defi-

Table 1
Solanum lycopersicum L. (cv. Micro-Tom) genotypes used in this study.

Genotype	Mature green fruit	Ripe fruit	Mutant gene function/phenotype	Tomato *locus*[a]	Reference
Micro-Tom (MT) *dwarf* (*d*) and *self-pruning* (*sp*) (control genotype)			*D* is a brassinosteroid biosynthesis enzyme encoding gene. The mutant allele reduces all organ sizes, except the fruits. *SP* regulates vegetative to reproductive switching of sympodial meristems. The mutant shows a determinate growth habit	Solyc02g089160 Solyc06g074350	Meissner et al. (1997), Martí et al. (2006), Bishop et al. (1999)
MT-*non ripening* (MT-*nor*)		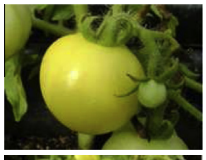	*NOR* is a NAC transcription factor. Mutant fruits do not ripe due to an alteration of the program that triggers climacteric ethylene biosynthesis	Solyc10g006880	Giovannoni et al. (1995)
MT-*ripening inhibitor* (MT-*rin*)			*RIN* is a MADS-box transcription factor. Mutants show an altered fruit ripening program, which fails to trigger climacteric respiration and ripening related ethylene biosynthesis	Solyc05g012020	Vrebalov et al. (2002)
MT-*green flesh* (MT-*gf*)			*gf* plants harbor a mutant allele of the STAY-GREEN1 protein encoding gene. The plants are deficient in chlorophyll degradation and present brownish fruits with green seed placental tissues	Solyc08g080090	Barry et al. (2008)
MT-*lutescent 1* (MT-*l*)	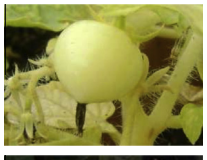	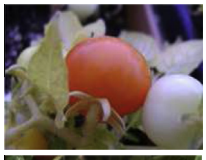	*L* is *locus* with unknown function. Mutant plants present non-pigmented ovaries and yellowish leaves	?	Jen (1974)
MT-*jasmonic acid insensitive 1-1* (MT-*jai*)			*JAI* is an F-box protein. Mutant plants are insensitive to JA and show delayed senescence of petals and styles, as well as glabrous ovaries	Solyc05g052620	Li et al. (2004)

[a] Sol Genomics Network (http://solgenomics.net/).

cient mutants, as well as following exogenous JA applications (Lim et al., 2007; Seltmann et al., 2010). JA treatment has been reported to promote climacteric fruit ripening by increasing ethylene production, accelerating Chl degradation and β-carotene biosynthesis (Fan et al., 1998). Moreover, the tomato JA-deficient mutants *spr2* and *def1* are impaired in lycopene accumulation and show reduced expression levels of lycopene biosynthetic genes (Liu et al., 2012). Although it has been proposed that JA might function independently of ethylene to promote ripening in tomato fruits, the underlying mechanism is still poorly understood (Liu et al., 2012). The tomato *jasmonic acid insensitive 1-1* (*jai*) mutant is, however, defective in the receptor component of the JA signal transduction pathway and fails to produce defense related compounds (Li et al., 2004), and although this mutant does not have an obvious senescence-related phenotype in vegetative tissues, it has delayed petal senescence and produces fruit lacking mature seeds (Li et al., 2004). Whether *JAI* also affects fruit ripening and ripening-related metabolic pathways remain to be determined.

Few studies have provided comprehensive insights into the regulation of the metabolic network that distribute common precursors towards isoprenoid compounds throughout fruit ripening. Described herein is an evaluation of how the impairment of different aspects of fruit development and ripening influence the metabolism of Chls, carotenoids and tocopherol and, consequently, fruit antioxidant capacity, by taking advantage of a collection of near isogenic tomato mutants.

2. Results and discussion

2.1. Transcriptional regulation of isoprenoid metabolism controls the pigment and antioxidant content of tomato fruits

During the transition from chloroplasts to chromoplasts in ripening tomato fruits, chlorophyll breakdown, carotenoid accumulation and tocopherol biosynthesis are tightly regulated, and the cross-talk between these isoprenoid branching pathways contributes to fruit nutritional quality (Vranová et al., 2012; Seymour et al., 2013a). In this current study, these metabolic interactions (Fig. 1) were explored by combining biochemical and gene expression analyses of ripening impaired, senescence-related and jasmonate insensitive tomato mutants (Table 1). The content of tocopherols, carotenoids and Chl were quantified in mature green (MG) and ripe (R) fruits from the MT-*rin*, MT-*nor*, MT-*gf*, MT-*l* and MT-*jai* mutants, as well as in the corresponding MT control (Fig. 2 and Table 2), using high-performance liquid chromatography (HPLC). Additionally, the expression patterns of twenty-five genes involved in the MEP (*DXS(1)*, *ISPE* and *GGDR*), post-chorismate SK (*ADH(1)*, *ADH(2)*, *TAT(1)*, *TAT(2)*, *HPPD(1)*, *HPPD(2)*) tocopherol-core (*VTE1*, *VTE2*, *VTE3(1)*, *VTE3(2)* and *VTE4*), carotenoid biosynthetic (*PDS*, *PSY(1)*, *PSY(2)*, *LCYβ*, *CYCβ*), Chl metabolism (*CHLG*, *CLH(1)*, *CLH(4)*, *PPH*, *PAO*) and phytol recycling (*VTE5*) pathways were assessed by qPCR (Figs. 1 and 3, Table S1 and Table S2).

Fruits from all the mutant and MT-wild type genotypes showed marked changes in levels of the analyzed isoprenoid-derived compounds during ripening (Fig. 2 and Table 2), with MT-*jai* showing the greatest number of metabolic changes, at both the MG and R stages, compared to the control. The MT-*rin* mutant showed the most highly altered gene expression profile, with significant differences in mRNA accumulation for all twenty-five analyzed genes in at least one of the tested ripening stages. In comparison, twenty and sixteen genes were differentially expressed in the fruits of the MT-*nor* and MT-*gf* mutant, respectively. Finally, the least altered expression profiles were seen in the MT-*l* and MT-*jai* mutants, for which only eight genes showed differential patterns of mRNA accumulation (Fig. 1 and Table S1). Thus, the more upstream the role of the mutated gene, in a regulatory context, the greater the impact on the transcriptional profile of the isoprenoid-biosynthesis related genes. This was especially evident when comparing the MT-*rin* and MT-*gf* genotypes, since while the former harbors a deletion in a ripening master transcription factor and shows a dramatically affected expression pattern in all the analyzed genes, the *gf* mutation affects a protein that regulates Chl degradation and, consequently, most of the genes with altered expression profiles are those associated with Chl metabolism (four out of six) and the VTE biosynthetic (four out of five) pathway (Fig. 1 and Table S1).

In order to evaluate the biochemical and gene expression profiles in an integrated manner, principal component analyses (PCA) were performed (Fig. 4). When the whole data set was analyzed, samples grouped by ripening stages. Samples from R fruits were scattered along PC1, while MG fruits were dispersed along the second component, suggesting that the metabolite and transcript profiles are more variable at the R than at the MG stage (Fig. 4A). When the same analysis was applied to data from the two stages separately, the first two dimensions explained approximately 53% of the variance for both the MG and R stages. At the MG stage, four groups were distinguished: MT-*l*, MT-*jai*, MT control and a cluster encompassing samples from the MT-*nor*, MT-*rin* and MT-*gf* mutants (Fig. 4B). However, at the R stage, all analyzed genotypes separated from each other by the first two PCA dimensions (Fig. 4C). It is notable that both metabolites and genes were found amongst the top eigenvectors, indicating that both types of variables contributed equally to sample separation. Moreover, when PCA were carried out exclusively with metabolites or gene expression profile data, samples were poorly separated (data not shown).

In the MT control genotype, the increased expression of the key enzyme encoding gene *DXS(1)* (Lois et al., 2000) and *PSY(1)* (Fraser et al., 2007), together with the transcriptional downregulation of *GGDR*, provides more isoprenoid intermediates for carotenoid biosynthesis (Fig. 3 and Table S1). Notwithstanding the transcriptional reduction of the phytol biosynthetic enzyme, tocopherol contents remained constant, suggesting the compensation via Chl breakdown, as proposed by Quadrana et al. (2013).

2.2. The MT-nor and MT-rin mutants

A number of transcription factors required for the initiation and promotion of tomato fruit ripening have been identified; however, the molecular mechanisms by which they interact are still largely unknown (Seymour et al., 2013b). *RIN* and *NOR* regulate the expression of genes involved in various aspects of fruit ripening, including carotenoid biosynthesis (Giovannoni et al., 1995; Vrebalov et al., 2002; Osorio et al., 2011; Martel et al., 2011; Fujisawa et al., 2013). The data herein show that R fruits from the MT-*rin* and MT-*nor* mutants had reduced levels of lycopene and higher levels of the photosynthetic xanthophyll neoxanthin than the control fruits (Table 2 and Fig. 5). Interestingly, these mutants were not deficient in β-carotene, and MT-*nor* actually accumulated more of this compound than the control at the R stage.

Publicly available chromatin immune precipitation (ChIP) assay data coupled with qPCR and/or large-scale gene expression analyses allowed retrieval of a catalog of genes that are directly or indirectly regulated by RIN (Martel et al., 2011; Fujisawa et al., 2011, 2012, 2013). The *DXS*, *ISPE* and geranylgeranyl diphosphate synthase (*GGPS*(2)) genes involved in the MEP pathway are all positively regulated in a RIN-dependent manner (Fujisawa et al., 2012, 2013). RIN also directly interacts with the promoter region of the *PSY(1)* gene, which constitutes the rate-limiting step of carotenoid biosynthesis (Fraser et al., 2007), favoring its transcrip-

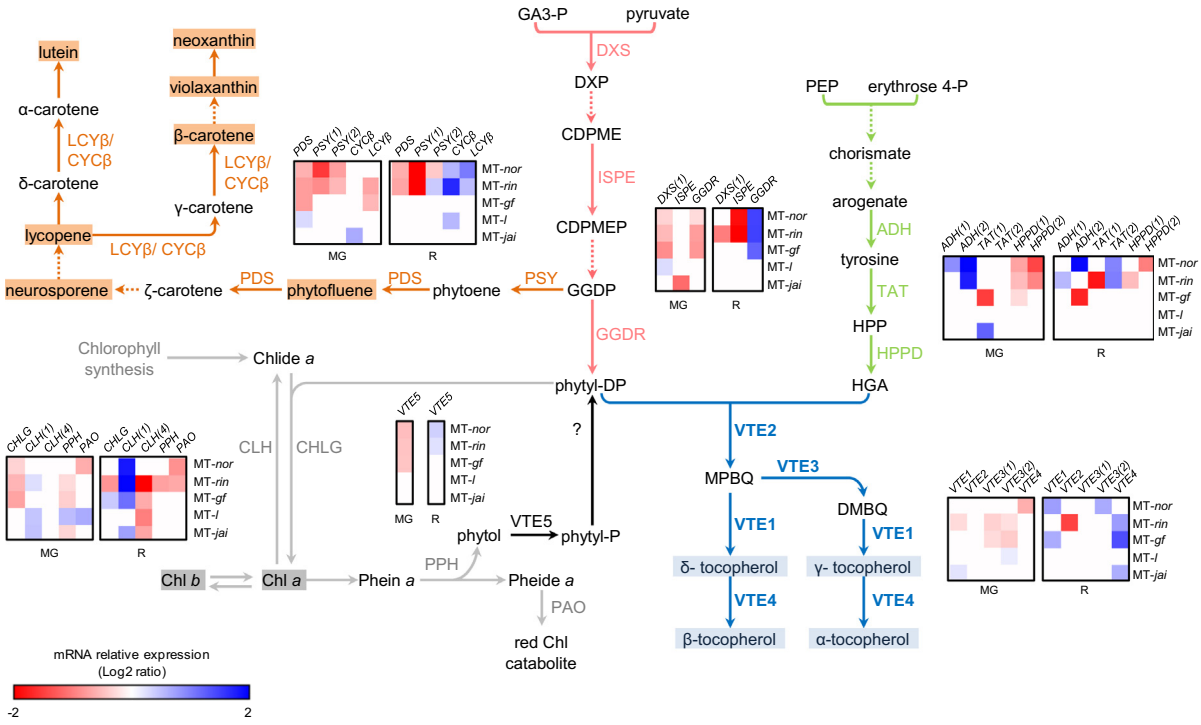

Fig. 1. Schematic view of the crosstalk between tocopherol, carotenoid and chlorophyll metabolism. The methyl erythritol phosphate, shikimate, tocopherol biosynthetic, carotenoid biosynthetic, chlorophyll metabolic and phytol recycling pathways are indicated in red, green, blue, orange, grey and black, respectively. The indicated enzyme encoding genes are those for which expression profiles were assayed. The genes are named according to the following abbreviations: 1-deoxy-D-xylulose-5-P synthase (*DXS*); 4-(cytidine 5′-diphospho)-2-C-methyl-D-erythritol kinase (*ISPE*); geranylgeranyl reductase (*GGDR*); arogenate dehydrogenase (*ADH*); tyrosine aminotransferase (*TAT*); 4-hydroxyphenylpyruvate dioxygenase (*HPPD*); homogentisate phytyl transferase (*VTE2*); 2,3-dimethyl-5-phytylquinol methyltransferase (*VTE3*); tocopherol cyclase (*VTE1*); γ-tocopherol C-methyl transferase (*VTE4*); phytoene synthase (*PSY*); phytoene desaturase (*PDS*); chloroplast-specific β-lycopene cyclase (*LCYβ*); chromoplast-specific β-lycopene cyclase (*CYCβ*); chlorophyll synthase (*CHLG*); chlorophyllase (*CLH*); pheophytinase (*PPH*); pheophorbide *a* oxygenase (*PAO*) and; phytol kinase (*VTE5*). Abbreviated intermediate metabolites are: glyceraldehyde 3-phosphate (GA3-P); 1-deoxy-D-xylulose-5-P (DXP); 4-(cytidine 5′-diphospho)-2-C-methyl-D-erythritol (CDPME); 2-phospho-4-(cytidine 5′-diphospho)-2-C-methyl-D-erythritol (CDPMEP); geranylgeranyl-2P (GG-2P); phosphoenolpyruvate (PEP); hydroxyphenylpyruvate (HPP); homogentisate (HGA); chlorophyllide *a* (Chlide *a*); chlorophyll *a* (Chl *a*); chlorophyll *b* (Chl *b*); pheophytin (Phein *a*); pheophorbide *a* (Pheide *a*); 2-methyl-6-geranylgeranylbenzoquinol (MPBQ) and; 2,3-dimethyl-6-geranylgeranylbenzoquinol (DMBQ). Highlighted metabolites were quantified. Gene expression profiles of each enzyme-encoding gene were measured by qPCR in samples of pericarp from mature green (MG) and ripe (R) tomato fruits ($n \geqslant 3$). Expression data are represented as $\log_2$ fold changes compared to the corresponding development stage of the Micro-Tom control by a color scale, where red and blue indicate statistically significant decreasing and increasing transcript levels ($p < 0.05$), respectively. (For interpretation of the references to colour in this figure legend, the reader is referred to the web version of this article.)

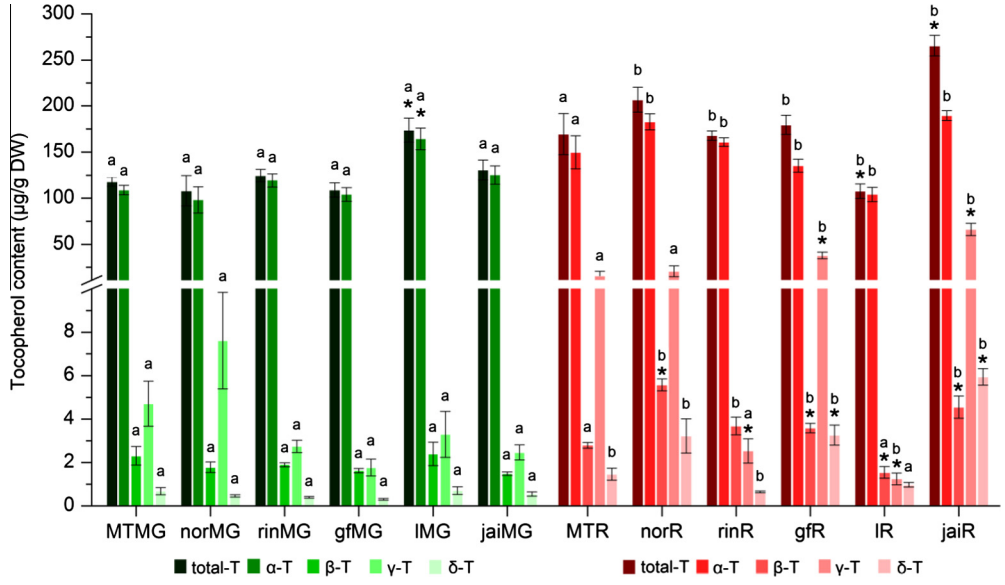

Fig. 2. Tocopherol content of the pericarp of fruits at the mature green (MG) and ripe (R) stages. Different letters indicate significant differences between both stages of the same genotype ($p < 0.05$). Asterisks denote significant differences compared to the corresponding stage of the Micro-Tom wild type control genotype ($p < 0.05$).

Table 2
Chlorophyll and carotenoid content of the pericarp of fruits at mature green (MG) and ripe (R) stages.

Genotype	Chlorophyll *a*	Chlorophyll *b*	Neoxanthin	Violaxanthin	Lutein	β-Carotene	Phytofluene	Neurosporene	Lycopene
Mature green									
MTMG	1.00 ± 0.06 *a*	1.00 ± 0.08 *a*	1.00 ± 0.07	1.00 ± 0.10	1.00 ± 0.11 *a*	1.00 ± 0.17 *a*	nd	nd	nd
MT-*nor*MG	0.95 ± 0.12 *a*	0.57 ± 0.08 *a*	1.08 ± 0.21 *a*	0.85 ± 0.11	0.92 ± 0.12 *a*	0.95 ± 0.13 *a*	nd	nd	nd
MT-*rin*MG	1.09 ± 0.09 *a*	1.09 ± 0.06 *a*	1.02 ± 0.05 *a*	1.09 ± 0.15	1.04 ± 0.06 *a*	1.14 ± 0.06 *a*	nd	nd	nd
MT-*gf*MG	1.27 ± 0.10 *a*	1.32 ± 0.12 *a*	1.46 ± 0.05**a*	1.23 ± 0.13	1.16 ± 0.07 *a*	1.25 ± 0.16 *a*	nd	nd	nd
MT-*l*MG	nd	nd	nd	nd	0.41 ± 0.02**a*	0.27 ± 0.03**a*	nd	nd	0.01 ± 0.00 *a*
MT-*jai*MG	1.65 ± 0.16**a*	1.53 ± 0.15**a*	1.77 ± 0.21*	2.97 ± 0.36**a*	1.33 ± 0.03 *a*	1.62 ± 0.04**a*	nd	nd	nd
Ripe									
MTR	0.02 ± 0.01 *b*	0.04 ± 0.00 *b*	nd	nd	0.80 ± 0.08 *a*	1.57 ± 0.15 *b*	1.00 ± 0.16	1.00 ± 0.03	1.00 ± 0.09
MT-*nor*R	0.34 ± 0.03**b*	0.25 ± 0.03**b*	0.43 ± 0.01**b*	nd	0.98 ± 0.12 *a*	2.71 ± 0.23**b*	nd	0.24 ± 0.01*	0.01 ± 0.00*
MT-*rin*R	0.38 ± 0.05**b*	0.36 ± 0.02**b*	0.48 ± 0.05**b*	nd	0.72 ± 0.05 *b*	1.32 ± 0.03 *a*	nd	0.21 ± 0.00*	nd
MT-*gf*R	0.45 ± 0.03**b*	0.56 ± 0.01**b*	0.84 ± 0.03**b*	nd	0.89 ± 0.04 *b*	1.62 ± 0.13 *a*	0.52 ± 0.12	0.90 ± 0.15	0.93 ± 0.24
MT-*l*R	nd	nd	nd	nd	0.89 ± 0.10 *b*	2.19 ± 0.36 *b*	1.04 ± 0.17	1.39 ± 0.24	1.67 ± 0.28 *b*
MT-*jai*R	0.11 ± 0.03**b*	0.22 ± 0.07**b*	nd	1.49 ± 0.35**b*	1.23 ± 0.05**a*	3.09 ± 0.39**b*	1.40 ± 0.21	1.07 ± 0.37	0.98 ± 0.11

Pigment levels in mature green (MG) and ripe (R) fruits. Data were normalized against MT-MG or MT-R. Asterisks denote significant differences from the corresponding stage of the MT wild type control genotype ($p < 0.05$). Different letters indicate significant differences between the stages of the same genotype ($p < 0.05$). nd indicates metabolite not detected.

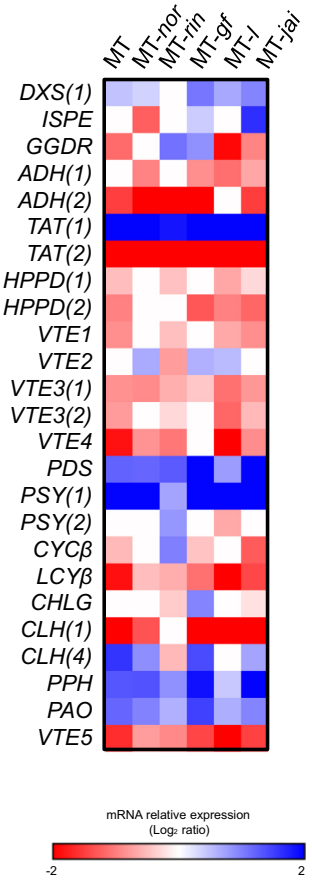

Fig. 3. Expression ratio between ripe (R) and mature green (MG) fruits within genotypes. The $\log_2$ of the expression ratios is indicated by a color scale where red and blue indicate statistically significant decreases and increases of transcript abundance ($p < 0.05$), respectively.

tion (Martel et al., 2011). Moreover, *NOR* expression is directly induced by RIN (Fujisawa et al., 2013), explaining the highly similar metabolic and gene expression profiles observed in MT-*rin* and MT-*nor*.

Here, lycopene deficiency in both mutants correlates with the reduced expression of *PSY(1)*, supporting previously reported observations (Kitagawa et al., 2005; Osorio et al., 2011; Martel et al., 2011). *PSY(1)* is the most highly expressed (The Tomato Genome Consortium, 2012) and functional studies demonstrated that this paralog has an essential role in carotenogenesis during tomato ripening (Fantini et al., 2013). Ripening mutants also showed significant decreased *PDS* mRNA levels (Fig. 5), as previously reported (Martel et al., 2011). Besides inhibition of the metabolic flux towards carotenoids, the lack of lycopene accumulation in R fruits of MT-*rin* and MT-*nor* is likely a consequence of *LCYβ* and *CYCβ* repression failure, resulting in higher amounts of the final product of the pathway, neoxanthin (Fig. 5). The low carotenoid content of R fruits of these two mutants could potentially result in more GGDP precursor being available for tocopherol biosynthesis. However, the downregulation of MEP pathway genes, *DXS* and *ISPE* (Fig. 1), could account for the maintenance of total tocopherol content in the ripening mutant fruits (Fig. 5). This result also supports the role for RIN as a transcriptional regulator of *DXS* and *ISPE* (Fujisawa et al., 2012, 2013). In addition, R fruits of the mutant genotypes showed higher levels of *GGDR* mRNA than the control (Fig. 5). As with *PDS*, for which the ChIP assays failed to detect an effect of RIN on expression (Martel et al., 2011), *GGDR* and the aforementioned *LCYβ* and *CYCβ* promoters contain putative CArG cis-elements, which are predicted RIN-binding motifs (Quadrana et al., 2013). Thus, these data suggest that NOR and RIN could be involved directly or indirectly in the down-regulation of *GGDR*, as well as the carotenoid genes *LCYβ* and *CYCβ*, at the onset of ripening (Fig. 1).

Regarding the SK pathway, in the MT control genotype, the transcriptional profile of *TAT(1)*, *TAT(2)*, *ADH(1)*, *ADH(2)*, *HPPD(1)* and *HPPD(2)* genes showed the same temporal fluctuation along ripening and similar relative expression within paralogs as that described for the Heinz cultivar (The Tomato Genome Consortium, 2012) (data not shown). However, in MT-*nor* and MT-*rin* mutants, these paralogs displayed a distinct pattern of alterations compared to the controls that apparently do not impact on homogentisate availability for tocopherol biosynthesis, suggesting a certain level of functional redundancy between paralogs (Fig. 5).

Both mutants are known to be deficient in Chl degradation and accordingly, it was observed that their R stage fruits retained approximately 30% of the total Chl *a* and *b* present at the MG stage (Table 2). Fruit de-greening is dependent on the activity of the Chl breakdown complex, which is regulated by the SGR protein, a key control point of Chl catabolism (Barry et al., 2008; Hu et al., 2011; Thomas and Ougham, 2014; Lira et al., 2014). The Chl degradation complex aggregates all the enzymes that catalyze the stepwise degradation of Chl to a primary fluorescent Chl catabolite,

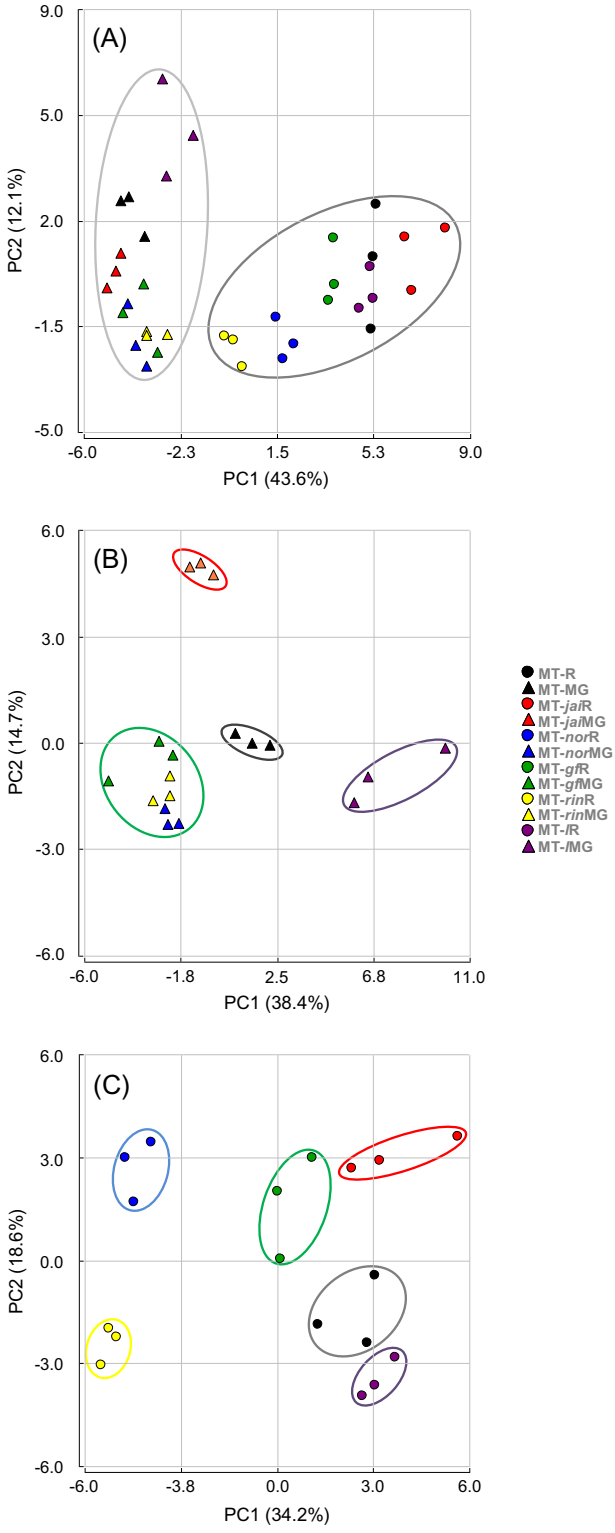

Fig. 4. Principal component analysis (PCA) of metabolic and gene expression profiles in the pericarp of tomato fruits. Metabolic and gene expression profiles of both mature green (MG) and ripe (R) (A); MG only (B); or R only (C) fruits subjected to PCA analysis.

including PPH and PAO (Sakuraba et al., 2012). *SGR1* is another direct target of RIN in tomato and its expression level is much higher in wild type than in the *rin* mutant throughout fruit development (Hu et al., 2011; Fujisawa et al., 2013), which might account in part for the Chl retention in R fruits of the MT-*nor* and MT-*rin* mutants (Fig. 5). Furthermore, these fruits also showed an apparent reduction in activity of the PAO-pathway, as indicated by a down-regulation of *PAO* and *PPH* expression (Fig. 5). Since MT-*gf*, an *sgr1* mutant, did not display the same patterns, it seems that NOR and RIN are directly or indirectly responsible for *PAO* and *PPH* expression reduction rather than being a consequence of SGR deficiency. Although *GGDR* is not down-regulated in MG or R fruits of the MT-*nor* and MT-*rin* mutants (Fig. 3), and *de novo* phytyl diphosphate biosynthesis might therefore not be repressed, the reduced levels of *CHLG* mRNA suggests that Chl biosynthesis is less active in the mutant fruits than in those of the control (Fig. 5). Furthermore, the maintenance of *CLH(1)* mRNA levels observed during MT-*nor* and MT-*rin* fruit development correlates with the Chl content as observed by Lira et al. (2014). Finally, *CLH(4)* has also been reported as a target of RIN (Fujisawa et al., 2012), and, in support of this, its expression was reduced in R fruits of the MT-*rin* mutant (Fig. 5).

In the context of tocopherol biosynthesis, the control fruits showed decreasing levels of *VTE3*, *VTE1* and *VTE4* expression throughout ripening, while *VTE2* remained constant (Fig. 3 and Table S2), which is in agreement with data previously reported by Quadrana et al. (2013). In contrast, MT-*rin* and MT-*nor* mutant fruits exhibited differing expression profiles for the tocopherol-core pathway genes (Figs. 1 and 3 and Table S1). For example, MT-*rin* R fruits showed a substantial repression of *VTE2* expression and a noticeable reduction of γ-tocopherol content compared to the control (Fig. 5), suggesting that NOR and RIN differentially modulate VTE biosynthesis. It was also noted that although levels of the Chl-derived phytol were lower in these ripening mutants, the maintenance of high expression levels of *GGDR* appear to be sufficient to the supply the prenyl side-chain for tocopherol production at the R stage (Fig. 5).

The findings here are consistent with previously published data concerning the signaling pathways regulated by RIN (Martel et al., 2011; Fujisawa et al., 2011, 2012, 2013). Furthermore, new evidence is provided regarding steps in the isoprenoid metabolism regulated by RIN and NOR in tomato fruits, as well as data promoting a better understanding of the differences observed in the metabolite profiles of the MT-*rin* and MT-*nor* mutant fruits.

2.3. The MT-*gf* mutant

The tomato *gf* mutant carries an amino acid substitution in an invariant residue of the ortholog of the Arabidopsis SGR protein (Barry et al., 2008). Since *gf* is not a knockout mutant, the activity of the Chl catabolic enzymes is not completely impaired in the mutant, and so the fruits retain detectable levels of Chl *a* and Chl *b* at the R stage (Table 2). The abnormal de-greening process correlates with multiple changes in the expression patterns of genes encoding enzymes involved in Chl and carotenoid metabolism, as well as in the MEP-, SK-, and tocopherol-core pathways. Interestingly, these results showed an effect of the *gf* mutation earlier than the onset of fruit ripening, as previously reported by Cheung et al. (1993). At the MG stage, the presence of the mutant allele resulted in the down-regulation of *DXS*, *GGDR*, *CHLG*, *PPH*, *VTE5*, *PDS*, *LCYβ*, *VTE3*, *TAT(1)* and *HPPD* transcripts (Fig. 5). Ripe fruits from the MT-*gf* mutant showed higher levels of *CLH(1)* mRNA compared to the control. This data correlates well with observations reported by Akhtar et al. (1999), that an accumulation of chlorophyllide *a* and *b* in R fruits from the *gf* mutant occurs following an increase in CLH activity. Interestingly, the increased levels of *GGDR* and *CHLG* mRNAs suggest that Chl biosynthesis remained active during late ripening in MT-*gf* mutant fruit (Fig. 5). It has been reported that Chl retention in *gf* is associated with the maintenance of chloroplast structure and photosynthesis related proteins, including the light-harvesting Chl *a*/*b*-binding proteins of photosystem II

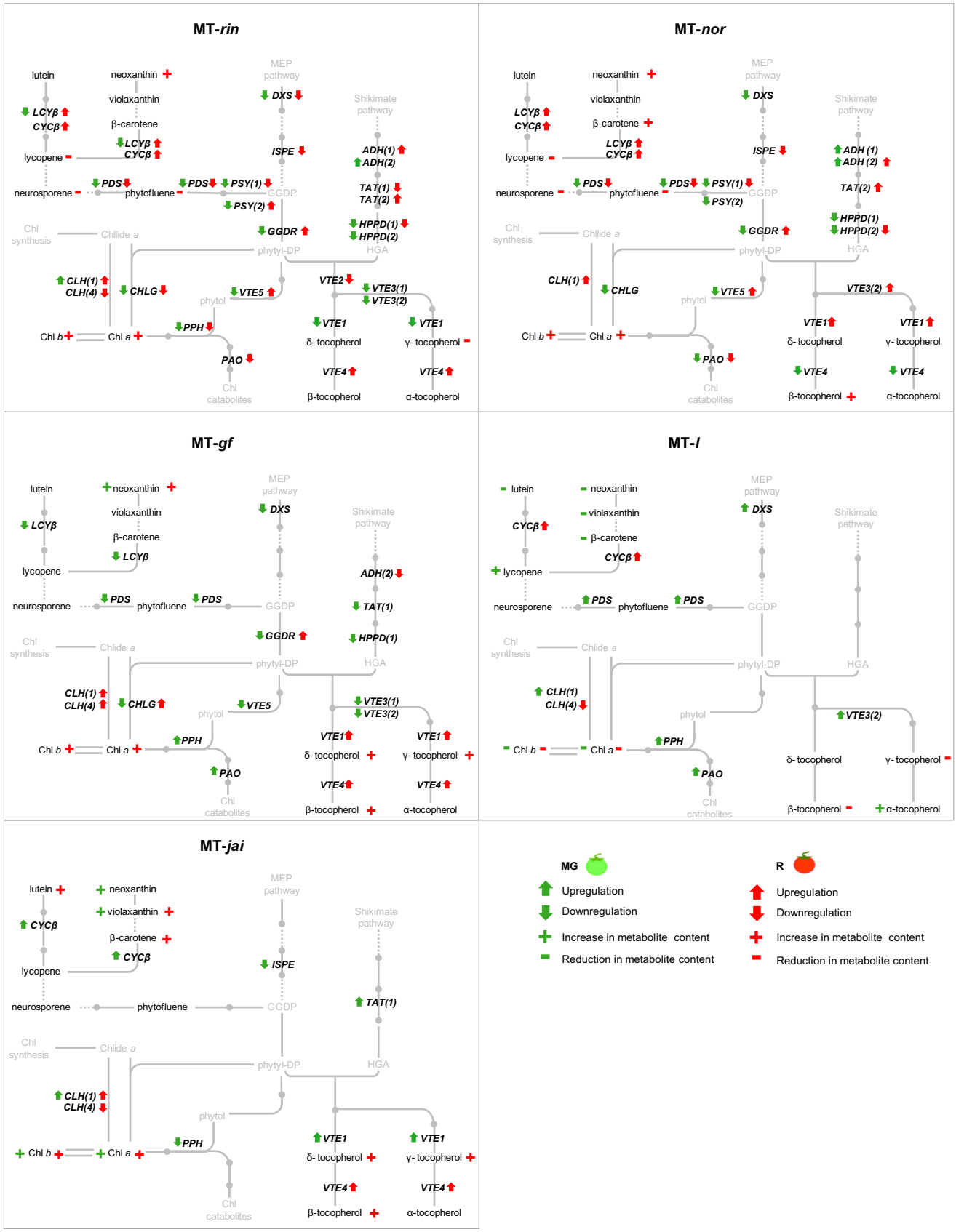

Fig. 5. Integrated view of the observed changes in chlorophyll, tocopherol and carotenoid content and gene transcriptional profiles for each tomato mutant compared with the corresponding stage of the Micro-Tom control. Gene expression (Table S1) and metabolite content changes (Fig. 2 and Table 2) are indicated by arrows and + or − signals, respectively. Mature green (MG) and ripe (R) stages are indicated by green and red colors, respectively.

and the small subunits of ribulose bisphosphate carboxylase/oxygenase, as well as their mRNAs (Cheung et al., 1993; Akhtar et al., 1999). It can, therefore, be inferred from these results that the Chl biosynthesis machinery is still functional in R stage fruits. Changes in transcriptional regulation of Chl biosynthetic genes were previously reported in the *Arabidopsis phytochrome A* mutant (Brouwer et al., 2014). Induced leaf yellowing in this mutant correlates to the repression of Chl biosynthesis associated genes rather than to an increase of its catabolism. Moreover, the maintenance of chloroplast structure is further evidence for the GGDR activity, since this enzyme is functional as long as it is anchored to membrane by light-harvesting-like protein LIL3 as previously reported (Tanaka et al., 2010; Takahashi et al., 2014).

The MT-*gf* mutant showed several alterations in tocopherol metabolism (Fig. 5). Despite the impairment in Chl catabolism, transcript levels of *VTE1* and *VTE4* increased at the R stage, a change is proposed to allow maintenance of total tocopherol contents equivalent to levels observed in the control fruit (Fig. 2). From MG to R, while fruits of the control genotype exhibited constant expression levels of *VTE2* and reduced levels of *VTE3(1)* and *(2)*, the corresponding MT-*gf* fruits showed an increase in *VTE2* and stable *VTE3(2)* mRNA levels, which suggests a corresponding increase in tocopherol biosynthesis (Fig. 3). Indeed, higher levels of β-, γ- and δ-tocopherol were detected in R MT-*gf* fruits compared to the control (Fig. 5). The perturbations in Chl and tocopherol accumulation do not seem to affect GGDP availability for carotenoid biosynthesis, since the carotenoid profile of the MT-*gf* mutant fruit resembles that of control fruits with the exception of neoxanthin (Table 2). The stronger up-regulation of *DXS(1)* and *PDS* expression from MG to R (Fig. 3 and Table S2) in this genotype may account in part for the maintenance of carbon precursors for the carotenoid pathway.

Recently, SGR1 has been shown to regulate lycopene and β-carotene biosynthesis in tomato fruits by direct interaction with PSY(1), thereby inhibiting its activity (Luo et al., 2013). Tomato *SGR1*-silenced lines showed *PSY(1)* mRNA accumulation and plastid conversion at the early stages of fruit ripening, resulting in increased lycopene and β-carotene contents in R fruits (Luo et al., 2013). In contrast, the *gf* mutation has no apparent effect on lycopene and β-carotene levels (Table 2), which is consistent with the study of Akhtar et al. (1999). One possible explanation for this apparent controversy is that the point mutation does not compromise the interaction with PSY. In addition, the accumulation of neoxanthin observed in these fruits (Fig. 5) might indicate that the Chl degradation deficiency partially impairs the disassembly of the photosynthetic apparatus. In agreement with this idea, it has been proposed that in the *sgr* mutant, Chl retention within the LHC shields its photosensitivity property; however the mechanism of energy dissipation under these conditions remains to be elucidated (Cheung et al., 1993; Sakuraba et al., 2012).

2.4. The MT-*l* mutant

The MT-*l* mutant contains a mutation in an unknown locus, resulting in premature leaf yellowing and albino fruits; however, Chl biosynthesis is not impaired in this genotype since at early stages of development the plant displays normal Chl production (Barry et al., 2012). The albino phenotype of the fruits is, however, consistent with the absence of Chls (Table 2).

The up-regulation of PAO-dependent Chl breakdown correlates with increased *PAO* and *PPH* mRNA levels (Fig. 1 and Table S1), suggesting that the lack of Chl in MG fruits is the result of accelerated degradation, rather than a reduction in biosynthesis. In addition to the lack of Chls, MG fruits from the MT-*l* mutant were also shown to have lower levels of violaxanthin and neoxanthin (Fig. 5), further implicating an impairment in the photosynthetic machinery.

Intriguingly, although *LCYβ* and *CYCβ* mRNA levels were comparable to those of the controls (Fig. 5), MG fruits from the MT-*l* mutants had detectable levels of lycopene, reduced β-carotene and lutein content and a lack of the xanthophylls neoxanthin and violaxanthin (Table 2). The observed increase in lycopene is in agreement with results previously reported by Jen (1974). The altered carotenoid profile exhibited by MT-*l* could be the consequence of another important regulatory mechanism involved in carotenoid accumulation, which relates to changes in storage and sequestration of carotenoids within various plastid structures (Cazzonelli and Pogson, 2011; Nogueira et al., 2013). Analysis of the chloroplasts from cotyledons of the *l* mutant have shown them to be impaired in thylakoid membrane development (Barry et al., 2012), and it may be that an equivalent alteration in fruit chloroplast structure of MT-*l* affects carotenoid accumulation. This chemotype, together with higher level of *DXS* mRNA, suggests increased metabolic flux towards tocopherol at the MG stage, which correlates with the observed increase in α- and total tocopherol levels compared to the control (Fig. 2).

At the R stage, transcriptional profile of the MEP pathway genes and carotenoid content of the MT-*l* fruits showed similar levels to control fruits. However, the dramatic phenotype of this Chl-deficient mutant was associated with a reduction in tocopherol levels at the R stage (Fig. 5). The absence of phytol derived from Chl breakdown is likely the cause of the observed reduction in β- and γ-tocopherol, which together resulted in a 35% decrease in total tocopherol content (Fig. 2). Although the ripening-impaired mutants (*nor* and *rin*) and the Chl retainer *gf* showed a reduction in the availability of Chl-derived phytol (Fig. 5), it can be proposed that the maintenance of high *GGDR* mRNA levels at the R stage in these mutants ensures sufficient levels of prenyl chain to maintain constant tocopherol levels. This compensatory mechanism might explain why seeds of *A. thaliana sgr* mutants show only a modest tocopherol reduction compared to wild type (Zhang et al., 2014). In contrast, in the MT-*l* mutant, besides the complete depletion of Chl-derived phytol, the *GGDR* expression showed a similar reduction to the control, further highlighting the importance of phytol derived from Chl degradation for tocopherol production during tomato fruit ripening (Quadrana et al., 2013).

2.5. The MT-*jai* mutant

The MT-*jai* mutant harbors a loss of function allele in the *CORONATINE-INSENSITIVE1* (*COI1*) *locus*, which encodes an F-box protein from the Skp/Cullin/F-box complex (SCF^{COI1}); a key component of the JA signaling pathway (Li et al., 2004). Upon perception of JA, COI1 promotes the degradation of the JAZ repressor (jasmonate ZIM-domain), thereby releasing transcription factors that will in turn activate JA-mediated responses (Wasternack and Hause, 2013). Although the role of JA in the regulation of plant fertility, secondary metabolism, and defense responses (Wasternack and Hause, 2013), including stress-induced leaf senescence (Kariola et al., 2005; Lira et al., 2014), has been widely reported, its role in fruit ripening remains poorly described (Fan et al., 1998).

During tomato fruit development, immediately prior to the MG jelly placenta stage, the endogenous concentration of JA peaks, causing an increase in ethylene production and accelerating chlorophyll degradation and carotenoid synthesis (Fan et al., 1998). In addition, it was shown that the JA-deficient mutants *spr2* and *def1* produce less ethylene at the breaker stage, accumulate less lycopene, and show a down-regulation of *DXS(1)*, *PSY* and *PDS* expression, while JA-overproducing transgenic plants show the opposite pattern (Liu et al., 2012). The JA and ethylene signaling pathways share a point of convergence, since JAZ also represses the EIN3/EIL1 protein, which is a positive regulator of ethylene responses, in a SCF^{COI1}-dependent manner (Zhu et al., 2011; Li

et al., 2013). N*EVER RIPE* (*nr*), an ethylene-insensitive mutant, shows a significant delay in fruit ripening does not reach the red ripe stage and exhibits very low levels of lycopene (Wilkinson et al., 1995; Osorio et al., 2011). However, the exogenous application of JA to *nr* partially rescues this phenotype, promoting the expression of lycopene biosynthetic genes and lycopene accumulation. These results indicate that even though JA and ethylene have a synergistic effect on tomato fruit ripening, JA signal transduction is not ethylene-dependent.

It was observed in this study that MT-*jai* fruits accumulated higher levels of Chl *a* and *b* at both ripening stages compared to the control (Table 2), and showed an increase in *CLH(1)* transcript abundance (Fig. 1). This observation is congruent with a role for *CLH(1)* in Chl recycling (Lira et al., 2014), although additional data are required to confirm this hypothesis. Interestingly, fruits from the JA insensitive mutant showed higher levels of β-carotene, violaxanthin and neoxanthin at the MG stage, and β-carotene, violaxanthin and lutein at the R stage than the controls (Fig. 5), which can be proposed to be a consequence of the higher accumulation of the fruit-specific *CYCβ* mRNA at the MG stage (Fig. 5). Moreover, in the transition from MG to R stages, the expected increase in *DXS*, *ISPE*, *PSY(1)* and *PDS* expression was stronger than in the control, which likely further contributed to the increased carotenoid content in R fruits (Fig. 3 and Table S2). Although these results may seem contradictory to those obtained for the *spr2* and *def1* mutants, they may in fact suggest the existence of a new variable in the complex regulatory network that controls fruit ripening. The absence of the JA peak before the MG stage in the *spr2* and *def1* mutants compromises ethylene production at the breaker stage, when the fruits exhibit the first visible trace of carotenoid accumulation. However, MT-*jai* is not defective in JA biosynthesis and the metabolic differences are primarily the results of the impairment of COI-dependent JA perception. In conclusion, the data herein suggest a COI-independent JA signaling pathway in tomato fruits, as previously proposed for *A. thaliana* (Caño-Delgado et al., 2003; Mueller and Berger, 2009).

Tocopherol levels also showed an increase in R fruits of MT-*jai* (Fig. 2), which are proposed to reflect, at least in part, the observed increases in *VTE1* and *TAT*(1) transcript levels at the MG and, *VTE4* at the R stage (Fig. 5). It has been demonstrated that fruit pericarp is an important source of carbon assimilate for determining seed metabolic profile (Lytovchenko et al., 2011). Chlorophyll degradation-derived phytol serves as an intermediate in tocopherol synthesis for seed VTE accumulation (Valentin et al., 2006). Since tocopherols are abundant in tomato seeds (Ellen et al., 2010) and, indeed, homozygous MT-*jai* fruits are seedless, the lack of seeds might contribute to the increased levels of tocopherols observed in the pericarp of these fruits (Fig. 5). The increase in β-carotene, violaxanthin and lutein (Table 2), together with increased VTE content suggest that the R fruits of the MT-*jai1* mutant have greater nutritional value and the highest antioxidant capacity of the tested genotypes (see below).

2.6. Analysis of antioxidant capacity

Profiling of pigment composition (Table 2) showed that the Chl and carotenoid contents of the mutant fruits were substantially different from those of the control. The Trolox equivalent antioxidant capacity (TEAC) showed little difference between the two ripening stages (Table 3) and the only genotypes with an increase in antioxidant capacity during ripening were the MT-*nor* and MT-*jai* mutants, and these two genotypes also showed an increase in β-carotene and total tocopherol levels. In contrast, MT-*l* fruits, which accumulated carotenes to the same degree as control fruits, but displayed a reduction in total-tocopherol, did not show a difference in antioxidant capacity between the MG and R stages. MT-*jai* was the only mutant with a higher total tocopherol content than the control at the R stage accompanied by an increase in antioxidant capacity, suggesting a major contribution of VTE to total antioxidant capacity in tomato fruits. Notably, R fruits from the MT-*jai* mutant also contained higher amounts of violaxanthin and lutein. Lutein has been reported to undergo the slowest degradation of the carotenoids in olive fruits and the radical species resulting from the molecular structure of lutein exhibit less propagation than those from β-carotene (Roca and Mínguez-Mosquera, 2001). It, therefore, cannot be disregarded that the potential effect of the increased lutein content is on the higher TEAC observed in MT-*jai* fruits. Underlining the influence of tocopherol on the antioxidant capacity of MT-*jai* fruits, previous studies have shown that the peroxyl radical scavenging capacity of β-carotene and lycopene is about one-tenth that of α-tocopherol, and the efficacy of lipid peroxidation inhibition is considerably smaller (Takashima et al., 2012). Moreover, the chemical species formed from carotenoids when they scavenge radicals are not stable, and may undergo several secondary reactions, thereby compromising the effects and efficacy of carotenoids as antioxidants (Takashima et al., 2012). The interactions between antioxidant compounds are complex and differences in the nature, concentrations and ratios in which they are present, are all important variables in defining antioxidant capacity (Gawlik-Dziki, 2012). A previous study of antioxidant capacity of lipophilic extracts obtained from different tomato varieties showed that tocopherol and β-carotene/lycopene act in a synergistic manner positively affecting antioxidant properties (Zanfini et al., 2010).

Table 3
Trolox equivalent antioxidant capacity (TEAC) in mature green (MG) and ripe (R) fruits.

Genotype	TEAC[a] Mean ± SE
MTMG	456.16 ± 39.27 *a*
MTR	641.62 ± 82.6 *a*
MT-*nor*MG	333.47 ± 16.2 *a*
MT-*nor*R	573.96 ± 83.67 *b*
MT-*rin*MG	403.32 ± 41.33 *a*
MT-*rin*R	534.59 ± 21.34 *a*
MT-*gf*MG	514.22 ± 87.38 *a*
MT-*gf*R	679.92 ± 24.25 *a*
MT-*l*MG	442.8 ± 49.66 *a*
MT-*l*R	525.97 ± 98.27 *a*
MT-*jai*MG	495.79 ± 35.88 *a*
MT-*jai*R	1,001.24 ± 152.96*b

Different letters indicate significant differences between stages of the same genotype ($p < 0.05$). Asterisks denote significant differences from the corresponding stage of the MT control genotype ($p < 0.05$).
[a] μmol of trolox equivalent/g of dry weight.

3. Concluding remarks

In this study, the metabolic network that links isoprenoid biosynthesis and recycling during ripening were explored in ripening impaired, senescence related and jasmonate insensitive tomato mutants. Although these pathways have been characterized in detail separately, few studies have addressed the potential cross-talk between isoprenoid derived pathways in a comprehensive manner.

The integrated analyses presented here revealed a remarkable plasticity of the interconnected Chl, carotenoid and tocopherol metabolic pathways, which is in part explained by the transcriptional regulation of the enzyme encoding genes from the corresponding pathways. This conclusion is supported by the fact that neither metabolites nor mRNA quantification alone discriminated between the mutant genotypes when non-parametric analyses

were applied (Fig. 4). The impact of transcriptional regulation on metabolite contents was proven by a weighted network analysis including mRNA, metabolites and TEAC quantification data (Fig. S1). The most striking difference in the topology of the constructed networks is that in all mutant genotypes, tocopherols appear highly connected with the other components, but this is not the case with the control genotype. This suggests that tocopherol composition is modified in the mutants diverting the isoprenoid metabolism, thereby keeping the antioxidant capacity constant. Network analyses also showed that in genotypes where Chl degradation is impaired, *GGDR* is connected with the tocopherol cluster but not the Chl cluster, supporting a putative role for this enzyme in supplying the prenyl side-chain for VTE biosynthesis, as discussed above. The analyses presented here indicate that transcription is a main regulatory mechanism of the isoprenoid metabolism; however, it is noted here that post-transcriptional and epigenetic regulation might also account for the complexity of this regulatory network (Martinis et al., 2013; Quadrana et al., 2014).

The biochemical analyses and gene expression profiles obtained from mutant-based resources contribute to a more detailed understanding of isoprenoid metabolism than was made possible by previously published data related to the RIN and NOR signal transduction pathways (Osorio et al., 2011; Martel et al., 2011; Fujisawa et al., 2013). Furthermore, this study provides insights into the effect of the *gf*, *l* and *jai* mutations on the regulatory networks that determine the composition of nutritionally important metabolites in tomato fruits. As a consequence of its wide distribution and high levels of global consumption, tomato is an important component of the human diet. The data presented here demonstrate that tocopherols make an important contribution to the antioxidant capacity of the tomato fruits, and suggest targets for future manipulation of their nutritional.

4. Experimental

4.1. Plant material

Seeds of *Solanum lycopersicum* L. (cv. Micro-Tom) (MT), and the mutants *lutescent 1* (*l*) (Barry et al., 2012), *green flesh* (*gf*) (Barry et al., 2008), *rin* (Vrebalov et al., 2002) and *nor* (Casals et al., 2012) in the MT background were produced in the Laboratory of Hormonal Control of Plant Development (www.esalq.usp.br/tomato). The mutations were introgressed by six successive backcrosses to the MT cultivar as the recurrent parent (BC6 generation), resulting in plants where at least 99% of the genome corresponds to MT. The *jai1-1* mutant (*jai*) in the MT background was kindly provided by Dr. Gregg Howe from Michigan State University. Due to the female sterility of *jai*, 1:1 segregating homozygous plants, which resulted from crosses between heterozygous MT-*jai* and homozygous *jai* (pollen donor), were screened in a methyl jasmonate (MeJA)-containing medium (Li et al., 2004; Campos et al., 2009). A brief description of all genotypes is presented in Table 1. Other than MT-*jai*, all the analyzed plants were homozygous for the mutations. The plants were grown in 8 l rectangular plastic pots containing a 1:1 mixture of commercial substrate (Plantmax HT, Eucatex, São Paulo, Brazil) and expanded vermiculite, supplemented with 1 g l^{-1} of NPK 10:10:10 and 4 g l^{-1} of dolomite limestone ($MgCO_3$ + $CaCO_3$). Plants were grown in a greenhouse under automatic irrigation (four times a day) in an average mean temperature of 25 °C; 11.5 h/13 h (winter/summer) photoperiod and 250–350 μmol m^{-2} s^{-1} of incident photo-irradiance. Fruit pericarp material (without placenta and locule walls) from the mature green (MG, jelly placenta), and ripe (R, placenta without Chl) stages was harvested. The MG stage was reached at approximately 35 days after anthesis (daa) for the MT, MT-*l*, MT-*gf*, MT-*jai* and MT-*rin* genotypes; and 38 daa for the MT-*nor* genotype. The R stage pericarp samples were collected at 45 daa for the MT, MT-*l*, MT-*gf* and MT-*jai* genotypes, 50 daa for the MT-*rin* mutant and at 54 daa for the MT-*nor* mutant. All samples were frozen in liq. N_2, homogenized and stored at −80 °C until further use. Samples were named with the mutant name followed by the ripening stage: MTMG, MTR, MT-*nor*MG, MT-*nor*R, MT-*rin*MG, MT-*rin*R, MT-*gf*MG, MT-*gf*R, MT-*l*MG, MT-*l*R, MT-*jai*MG and MT-*jai*R (Table 1).

4.2. Tocopherol and pigment quantification by HPLC

Tocopherols and pigments were extracted as described in Almeida et al. (2011) and the samples adjusted to a final volume (4 ml). For tocopherol analysis, aliquots (3 ml) were dried under N_2 and dissolved in a mobile phase (200 μl) composed of hexane/tert-butyl methyl ether (90:10). Chromatography was carried out on a Hewlett–Packard series 1100 HPLC system coupled with a fluorescence detector (Agilent Technologies series 1200) on a normal-phase column (LiChrosphere® 100 Diol Si (250 mm × 4.0 mm, 5 μm; Agilent Technologies, Germany) at room temperature, with the mobile phase running isocratically at 1 ml min^{-1}. Eluted compounds were detected by excitation at 295 nm and quantifying their fluorescence at 330 nm.

For pigment analysis, aliquots (500 μl) of extract were dried under N_2 and dissolved in MeOH: EtOAC (500 μl, 50:50, v/v). Chromatography was performed with an Agilent 1200 Series HPLC system coupled with a Diode Array Detector on a reversed phase column (Zorbax Eclipse Plus C18 (150 mm × 4.6 mm, 5 μm; Agilent Technologies, USA) at room temperature using a 0.6 ml min^{-1} flow rate. The elution was performed with a linear gradient of 100% solvent A (CH_3CN/MeOH/Tris buffer [0.1 M, pH 8] in a 72:8:3 ratio) to 100% solvent B (MeOH/EtOAC in a 68:32 ratio) from 0 to 25 min, followed by 10 min with 100% solvent B. For column equilibration, the mobile phase was returned to 100% solvent A and maintained for 5 min. Throughout the chromatography run, the eluate was monitored continuously from 200 to 800 nm. Lutein, β-carotene, and lycopene were quantified at 440 nm by comparison with an external standard (Sigma–Aldrich Chemical Co., USA). Phytofluene, Chl *a* and Chl *b* were quantified based on their absorption coefficient: ε1% (348 nm) = 1577, ε(431 nm) = 95.99 cm^{-1} mM^{-1} and ε(430 nm) = 57.43 cm^{-1} mM^{-1}, respectively. These compounds were expressed as μg g^{-1} of dry weight. Neurosporene, violaxanthin, neoxanthin and pheophytin were identified and quantified at 440 nm and expressed as area (mAU*seg) per g of fruit dry weight.

4.3. Trolox equivalent antioxidant capacity (TEAC)

The antioxidant capacity of the tocopherol and pigment extracts was assayed as previously described (Re et al., 1999), with minor modifications. The pre-formed radical monocation of 2,2′-azinobis-(3-ethylbenzothiazoline-6-sulfonic acid) ($ABTS^{\cdot+}$) was produced by oxidation of 7 mM ABTS with potassium persulphate (2.45 mM final concentration) dissolved in H_2O. The mixture was placed in the dark at room temperature for 12–16 h before use, and the $ABTS^{\cdot+}$ solution was diluted with EtOH and equilibrated at 30 °C to an absorbance of 0.70 ± 0.02 at 734 nm. Aliquots of 25 μL extract or Trolox standard was mixed with 1 ml of diluted $ABTS^{\cdot+}$ solution, vortexed for 10 s, and the absorbance measured at 734 nm after 4 min at 30 °C. Values were obtained by interpolating the absorbance on a calibration curve using Trolox (0.03–0.50 mM) and were expressed as μmol of Trolox equivalent per g of dry weight. All samples were analyzed in triplicate.

4.4. Quantitative polymerase chain reaction (qPCR)

RNA extraction and qPCR reactions were performed as described by Quadrana et al. (2013). Annotated gene function and primer sequences are described in Table S3. All reactions were performed using two technical replicates and at least three biological replicates. mRNA levels were quantified using a 7500 Real-Time PCR system (Applied Biosystems) and SYBR Green Master Mix (Applied Biosystems). Data were analyzed using the LinRegPCR software package (Ruijter et al., 2009) to obtain Ct values and to calculate primer efficiency. Expression values were normalized to the mean of two constitutively expressed genes, *CAC* and *EXPRESSED* (Quadrana et al., 2013). A permutation test lacking sample distribution assumptions (Pfaffl et al., 2002) was applied to detect statistical differences ($p < 0.05$) in expression levels between mutants and the control using the algorithms in the fgStatistics software package (Di Rienzo, 2009).

4.5. Data analysis and statistics

Data obtained from tocopherol, pigment and antioxidant capacity measurements were analyzed using the InfoStat software package (Di Rienzo et al., 2011). When a data set showed homoscedasticity, an ANOVA test followed by a Tukey test ($p < 0.05$) was used to compare genotypes and fruit developmental stages. In the absence of homoscedasticity, a non-parametric ANOVA test was performed by applying the Kruskal–Wallis test ($p < 0.05$). All values represent the mean of at least four biological replicates.

PCA analyses were performed using the InfoStat software package and heatmaps were produced using GENE-E (http://www.broadinstitute.org/cancer/software/GENE-E/). Network construction and analyses was performed with expression and metabolite data using the WGCNA R software package (Zhang and Horvath, 2005). A signed network with threshold power (b) = 6 was produced according to Zhang and Horvath (2005) and Horvath (personal communication). The network was constructed with genes and metabolites presenting node connectivities $\geqslant 0.65$ by using an edge-weighted force-directed layout incorporated in the Cytoscape software package (Shannon et al., 2003).

Acknowledgements

JA and BSL were recipients of a FAPESP fellowship. MR and LEPP were funded by a fellowship from CNPq. This work was partially supported by grants from FAPESP (Brazil), CNPq (Brazil) and USP (Brazil). The authors wish to thank Dr. Gregg A. Howe (Michigan State University) for supplying the *jai* mutant in the MT background and Dr. Roger Chetelat (Tomato Genetics Resource Center, Davis, USA) who provided the *l*, *nor*, *rin* and *gf* mutants in different backgrounds. We thank PlantScribe (www.plantscribe.com) for carefully editing this manuscript.

Appendix A. Supplementary data

Supplementary data associated with this article can be found, in the online version, at http://dx.doi.org/10.1016/j.phytochem.2014.11.007.

References

Akhtar, M.S., Goldschmidt, E.E., John, I., Rodoni, S., Matile, P., Grierson, D., 1999. Altered patterns of senescence and ripening in gf, a stay-green mutant of tomato (*Lycopersicon esculentum* Mill.). J. Exp. Bot. 50, 1115–1122.

Almeida, J., Quadrana, L., Asís, R., Setta, N., De Godoy, F., Bermúdez, L., Otaiza, S.N., Corrêa da Silva, J.V., Fernie, A.R., Carrari, F., Rossi, M., 2011. Genetic dissection of vitamin E biosynthesis in tomato. J. Exp. Bot. 62, 3781–3798.

Barry, C.S., Aldridge, G.M., Herzog, G., Ma, Q., McQuinn, R.P., Hirschberg, J., Giovannoni, J.J., 2012. Altered chloroplast development and delayed fruit ripening caused by mutations in a zinc metalloprotease at the *lutescent2* locus of tomato. Plant Physiol. 159, 1086–1098.

Barry, C.S., McQuinn, R.P., Chung, M.Y., Besuden, A., Giovannoni, J.J., 2008. Amino acid substitutions in homologs of the STAY-GREEN protein are responsible for the *green-flesh* and *chlorophyll retainer* mutations of tomato and pepper. Plant Physiol. 147, 179–187.

Bishop, G.J., Nomura, T., Yokota, T., Harrison, K., Noguchi, T., Fujioka, S., Takatsuto, S., Jones, J.D.G., Kamiya, Y., 1999. The tomato DWARF enzyme catalyses C-6 oxidation in brassinosteroid biosynthesis. Proc. Natl. Acad. Sci. U.S.A. 96, 1761–1766.

Bramley, P.M., 2002. Regulation of carotenoid formation during tomato fruit ripening and development. J. Exp. Bot. 53, 2107–2113.

Brigelius-Flohé, R., Kelly, F.J., Salonen, J.T., Neuzil, J., Zingg, J.M., Azzi, A., 2002. The European perspective on vitamin E: current knowledge and future research. Am. J. Clin. Nutr. 76, 703–716.

Brouwer, B., Gardestrom, P., Keech, O., 2014. In response to partial plant shading, the lack of phytochrome A does not directly induce leaf senescence but alters the fine-tuning of chlorophyll biosynthesis. J. Exp. Bot.. http://dx.doi.org/10.1093/jxb/eru060.

Campos, M.L., Almeida, M., Rossi, M.L., Martinelli, A.P., Junior, C.G.L., Figueira, A., Rampelotti-Ferreira, F.T., Vendramim, J.T., Benedito, V.A., Peres, L.E.P., 2009. Brassinosteroids interact negatively with jasmonates in the formation of anti-herbivory traits in tomato. J. Exp. Bot. 60, 4347–4361.

Caño-Delgado, A., Penfield, S., Smith, C., Catley, M., Bevam, M., 2003. Reduced cellulose synthesis invokes lignification and defense responses in *Arabidopsis thaliana*. Plant J. 34, 351–362.

Casals, J., Pascual, L., Canizares, J., Cebolla-Cornejo, J., Casanas, F., Nuez, F., 2012. Genetic basis of long shelf life and variability into Penjar tomato. Genet. Resour. Crop Evol. 59, 219–229.

Cazzonelli, C.I., Pogson, B.J., 2011. Source to sink: regulation of carotenoid biosynthesis in plants. Trends Plant Sci. 15, 266–274.

Cheung, A.Y., McNellis, T., Piekos, B., 1993. Maintenance of chloroplast components during chromoplast differentiation in the tomato mutant *green flesh*. Plant Physiol. 101, 1223–1229.

Dall'Osto, L., Lico, C., Alric, J., Giuliano, G., Havaux, M., Bassi, R., 2006. Lutein is needed for efficient chlorophyll triplet quenching in the major LHCII antenna complex of higher plants and effective photoprotection in vivo under strong light. BMC Plant Biol. 6, 32.

DellaPenna, D., Pogson, B.J., 2006. Vitamin synthesis in plants: tocopherols and carotenoids. Annu. Rev. Plant Biol. 57, 711–738.

Di Rienzo, J.A., Casanoves, F., Balzarini, M.G., Gonzalez, L., Tablada, M., Robledo, C.W., 2011. InfoStat Versión 2011. FCA, Universidad Nacional de Córdoba, Argentina, <http://www.infostat.com.ar/>.

Di Rienzo, J.A., 2009. Statistical Software for the Analysis of Experiments of Functional Genomics. RDNDA, Argentina, <http://sites.google.com/site/fgStatistics/>.

Egea, I., Bian, W., Barsan, C., Jauneau, A., Pech, J.C., Latché, A., Li, Z.G., Chervin, C., 2011. Chloroplast to chromoplast transit ion in tomato fruit: spectral confocal microscopy analyses of carotenoids and chlorophylls in isolated plastids and time-lapse recording on intact live tissue. Ann. Bot. (Lond.) 108, 291–297.

Ellen, F.J., Moser, J.K., Kenar, J.A., Taylor, S.L., 2010. Extraction and analysis of tomato seed oil. J. Am. Oil Chem. Soc. 87, 755–762.

Fan, X., Mattheis, J.P., Fellman, J.K., 1998. A role for jasmonates in climacteric fruit ripening. Planta 204, 444–449.

Fantini, E., Falcone, G., Frusciante, S., Giliberto, L., Giuliano, G., 2013. Dissection of tomato lycopene biosynthesis through virus-induced gene silencing. Plant Physiol. 163, 986–998.

Fraser, P.D., Enfissi, E.M., Halket, J.M., Truesdale, M.R., Yu, D., Gerrish, C., Bramley, P.M., 2007. Manipulation of phytoene levels in tomato fruit: effects on isoprenoids, plastids, and intermediary metabolism. Plant Cell 19, 3194–3211.

Fujisawa, M., Nakano, T., Ito, Y., 2011. Identification of potential target genes for the tomato fruit-ripening regulator *RIN* by chromatin immunoprecipitation. BMC Plant Biol. 11, 26.

Fujisawa, M., Nakano, T., Shima, Y., Ito, Y., 2013. A large-scale identification of direct targets of the tomato MADS box transcription factor *RIPENING INHIBITOR* reveals the regulation of fruit ripening. Plant Cell 25, 371–386.

Fujisawa, M., Shima, Y., Higuchi, N., Nakano, T., Koyama, Y., Kasumi, T., Ito, Y., 2012. Direct targets of the tomato-ripening regulator RIN identified by transcriptome and chromatin immunoprecipitation analyses. Planta 235, 1107–1122.

Gawlik-Dziki, U., 2012. Changes in the antioxidant activities of vegetables as a consequence of interactions between active compounds. J. Funct. Foods 4, 872–882.

Giovannoni, J., Noensie, E.N., Ruezinsky, D.M., Lu, X., Tracy, S.L., Ganal, M.W., Martin, G.B., Pillen, K., Alpert, K., Tanksley, S.D., 1995. Molecular genetic analysis of the ripening-inhibitor and non-ripening loci of tomato: a first step in genetic map-based cloning of fruit ripening genes. Mol. Gen. Genet. 248, 195–206.

Giovannoni, J.J., 2004. Genetic regulation of fruit development and ripening. Plant Cell 16, S170–180.

Hörtensteiner, S., 2009. Stay-green regulates chlorophyll and chlorophyll-binding protein degradation during senescence. Trends Plant Sci. 14, 155–162.

Hu, Z.L., Deng, L., Yan, B., Pan, Y., Luo, M., Chen, X.Q., Hu, T.Z., Chen, G.P., 2011. Silencing of the *LeSGR1* gene in tomato inhibits chlorophyll degradation and exhibits a stay-green phenotype. Biol. Plant. 55, 27–34.
Ischebeck, T., Zbierzak, A.M., Kanwischer, M., Dörmann, P., 2006. A salvage pathway for phytol metabolism in Arabidopsis. J. Biol. Chem. 281, 2470–2477.
Jen, J.J., 1974. Carotenoids of yellow and red lutescent tomatoes. J. Agric. Food Chem. 22, 908–910.
Kariola, T., Brader, G., Li, J., 2005. Chlorophyllase 1, a damage control enzyme, affects the balance between defense pathways in plants. Plant Cell 17, 282–294.
Kitagawa, M., Ito, H., Shiina, T., Nakamura, N., Inakuma, T., Kasumi, T., Ishiguro, Y., Yabe, K., Ito, Y., 2005. Characterization of tomato fruit ripening and analysis of gene expression in F1 hybrids of the ripening inhibitor (rin) mutant. Physiol. Planta 123, 331–338.
Krieger-Liszkay, A., Trebst, A., 2006. Tocopherol is the scavenger of singlet oxygen produced by the triplet states of chlorophyll in the PSII reaction centre. J. Exp. Bot. 57, 1677–1684.
Li, L., Zhao, Y., McCaig, B.C., Wingerd, B.A., Wang, J., Whalon, M.E., Pichersky, E., Howe, G.A., 2004. The tomato homolog of CORONATINE-INSENSITIVE1 is required for the maternal control of seed maturation, jasmonate-signaled defense responses, and glandular trichome development. Plant Cell 16, 126–143.
Li, Z., Peng, J., Wen, X., Guo, H., 2013. Ethylene-insensitive3 is a senescence-associated gene that accelerates age-dependent leaf senescence by directly repressing miR164 transcription in Arabidopsis. Plant Cell 25, 3311–3328.
Lim, P.O., Kim, H.J., Nam, H.G., 2007. Leaf senescence. Annu. Rev. Plant Biol. 58, 115–136.
Lira, B., de Setta, N., Rosado, D., Almeida, J., Freschi, L., Rossi, M., 2014. Plant degreening: evolution and expression of tomato (*Solanum lycopersicum*) dephytylation enzymes. Gene, <http://dx.doi.org/10.1016/j.gene.2014.05.051/>.
Lois, L.M., Rodríguez-Concepción, M., Gallego, F., Campos, N., Boronat, A., 2000. Carotenoid biosynthesis during tomato fruit development: regulatory role of 1-deoxy-D-xylulose 5-phosphate synthase. Plant J. 22, 503–513.
Lytovchenko, A., Eickmeier, I., Pons, C., Osorio, S., Szecowka, M., Lehmberg, K., Stephanie Arrivault, S., Takayuki, T., Pineda, B., Anton, M.T., Hedtke, B., Lu, Y., Fisahn, J., Bock, R., Stitt, M., Grimm, B., Granell, A., Fernie, A.F., 2011. Tomato fruit photosynthesis is seemingly unimportant in primary metabolism and ripening but plays considerable role in seed development. Plant Physiol. 157, 1650–1663.
Liu, L., Wei, J., Zhang, M., Zhang, L., Li, C., Wang, Q., 2012. Ethylene independent induction of lycopene biosynthesis in tomato fruits by jasmonates. J. Exp. Bot. 63, 5751–5761.
Luo, Z., Zhang, J., Li, J., Yang, C., Wang, T., Ouyang, B., Li, H., Giovannoni, J., Ye, Z., 2013. A STAY-GREEN protein SlSGR1 regulates lycopene and β-carotene accumulation by interacting directly with SlPSY1 during ripening processes in tomato. New Phytol. 198, 442–452.
Martel, C., Vrebalov, J., Tafelmeyer, P., Giovannoni, J., 2011. The tomato MADS-box transcription factor ripening inhibitor interacts with promoters involved in numerous ripening processes in a colorless nonripening-dependent manner. Plant Physiol. 157, 1568–1579.
Martí, E., Gisbert, C., Bishop, G.J., Dixon, M.S., Garcia-Martinez, J.L., 2006. Genetic and physiological characterization of tomato cv. Micro-Tom. J. Exp. Bot. 57, 2037–2047.
Martinis, J., Glauser, G., Valimareanu, S., Kessler, F., 2013. A chloroplast ABC1-like kinase regulates vitamin E metabolism in *Arabidopsis thaliana*. Plant Physiol. 162, 652–662.
Meissner, R., Jacobson, Y., Melamed, S., Levyatuv, S., Shalev, G., Ashri, A., Elkind, Y., Levy, A., 1997. A new model system for tomato genetics. Plant J. 12, 1465–1472.
Mueller, M.J., Berger, S., 2009. Reactive electrophilic oxylipins: pattern recognition and signalling. Phytochemistry 70, 1511–1521.
Niki, E., Traber, M.G., 2012. History of vitamin E. Ann. Nutr. Metab. 61, 207–212.
Nogueira, M., Mora, L., Enfissi, E.M.A., Bramley, P.M., Fraser, P.D., 2013. Subchromoplast sequestration of carotenoids affects regulatory mechanisms in tomato lines expressing different carotenoid gene combinations. Plant Cell 25, 4560–4579.
Osorio, S., Alba, R., Damasceno, C.M.B., Lopez-Casado, G., Lohse, M., Zanor, M.I., Tohge, T., Usadel, B., Rose, J.K.C., Fei, Z., Giovannoni, J.J., Fernie, A.R., 2011. Systems biology of tomato fruit development: combined transcript, protein, and metabolite analysis of tomato transcription factor (nor, rin) and ethylene receptor (nr) mutants reveals novel regulatory interactions. Plant Physiol. 157, 405–425.
Park, S.Y., Yu, J.W., Park, J.S., Li, J., Yoo, S.C., Lee, N.Y., Lee, S.K., Jeong, S.W., Seo, H.S., Koh, H.J., Jeon, J.S., Park, Y.I., Paek, N.C., 2007. The senescence-induced staygreen protein regulates chlorophyll degradation. Plant Cell 19, 1649–1664.
Perez-Fons, L., Wells, T., Corol, D.I., Ward, J.L., Gerrish, C., Beale, M.H., Seymour, G.B., Bramley, P.M., Fraser, P.D., 2014. A genome-wide metabolomic resource for tomato fruit from *Solanum pennellii*. Sci. Rep. 4, 1–8.
Pfaffl, M.W., Horgan, G.W., Dempfle, L., 2002. Relative expression software tool (REST) for group-wise comparison and statistical analysis of relative expression results in real-time PCR. Nucleic Acids Res. 30, e36.
Quadrana, L., Almeida, J., Otaiza, S.N., Duffy, T., Corrêa da Silva, J.V., de Godoy, F., Asís, R., Bermúdez, L., Fernie, A.R., Carrari, F., Rossi, M., 2013. Transcriptional regulation of tocopherol biosynthesis in tomato. Plant Mol. Biol. 81, 309–325.
Quadrana, L., Almeida, J., Asís, R., Duffy, T., Dominguez, P.G., Bermúdez, L., Conti, G., da Silva, J.V.C., Colot, V., Asurmendi, S., Fernie, A.R., Rossi, M., Carrari, F., 2014. Natural occurring epialleles determine vitamin E accumulation in tomato fruits. Nat. Commun.. http://dx.doi.org/10.1038/ncomms5027.
Re, R., Pellegrini, N., Proteggente, A., Pannala, A., Yang, A., Rice-Evans, C., 1999. Antioxidant activity applying an improved ABTS radical cation decolorization assay. Free Radical Biol. Med. 26, 1231–1237.
Roca, M., Mínguez-Mosquera, M.I., 2001. Changes in chloroplast pigments of olive varieties during fruit ripening. J. Agric. Food Chem. 49, 832–839.
Ruijter, J.M., Ramakers, C., Hoogaars, W.M., Karlen, Y., Bakker, O., van den Hoff, M.J., Moorman, A.F.M., 2009. Amplification efficiency: linking baseline and bias in the analysis of quantitative PCR data. Nucleic Acids Res. 37, e45.
Sakuraba, Y., Schelbert, S., Park, S.Y., Han, S.H., Lee, B.D., Andrès, C.B., Kessler, F., Hörtensteiner, S., Paek, N.C., 2012. STAY-GREEN and chlorophyll catabolic enzymes interact at light-harvesting complex II for chlorophyll detoxification during leaf senescence in Arabidopsis. Plant Cell 24, 507–518.
Seltmann, M.A., Stingl, N.E., Lautenschlaeger, J.K., Krischke, M., Mueller, M.J., Berger, S., 2010. Differential impact of lipoxygenase2 and jasmonates on natural and stress-induced senescence in *Arabidopsis thaliana*. Plant Physiol. 152, 1940–1950.
Seybold, C., Fröhlich, K., Bitsch, R., Otto, K., Böhm, V., 2004. Changes in contents of carotenoids and vitamin E during tomato processing. J. Agric. Food Chem. 52, 7005–7010.
Seymour, G., Taylor, J., Tucker, G. (Eds.), 1993. Biochemistry of fruit ripening. Chapman and Hall, London, 442 pp.
Seymour, G.B., Chapman, N.H., Chew, B.L., Rose, J.K., 2013a. Regulation of ripening and opportunities for control in tomato and other fruits. Plant Biotech. J. 11, 269–278.
Seymour, G.B., Østergaard, L., Chapman, N.H., Knapp, S., Martin, C., 2013b. Fruit development and ripening. Annu. Rev. Plant Biol. 64, 219–241.
Shannon, P., Markiel, A., Ozier, O., Baliga, N.S., Wang, J.T., Ramage, D., Amin, N., Schwikowski, B., Ideker, T., 2003. Cytoscape: a software environment for integrated models of biomolecular interaction networks. Genome Res. 13, 2498–2504.
Takahashi, K., Takabayashi, A., Tanaka, A., Tanaka, R., 2014. Functional analysis of light-harvesting-like protein 3 (LIL3) and its light-harvesting chlorophyll-binding motif in Arabidopsis. J. Biol. Chem. 289, 987–999.
Takashima, M., Shichiri, M., Hagihara, Y., Yoshida, Y., Niki, E., 2012. Capacity of peroxyl radical scavenging and inhibition of lipid peroxidation by β-carotene, lycopene, and commercial tomato juice. Food Funct. 3, 1153–1160.
Tanaka, R., Rothbart, M., Oka, S., Takabayashi, A., Takahashi, K., Shibata, M., Myouga, F., Motohashi, R., Shinozaki, K., Grimm, B., Tanaka, A., 2010. LIL3, a light-harvesting-like protein, plays an essential role in chlorophyll and tocopherol biosynthesis. Proc. Natl. Acad. Sci. U.S.A. 107, 16721–16725.
The Tomato Genome Consortium, 2012. The tomato genome sequence provides insights into fleshy fruit evolution. Nature 485, 635–641.
Thomas, H., Ougham, H., 2014. The stay-green trait. J. Exp. Bot.. http://dx.doi.org/10.1093/jxb/eru037.
Trebst, A., 2003. Function of β-carotene and tocopherol in photosystem II. Z. Naturforsch. C. 58, 609–620.
Valentin, H.E., Lincoln, K., Moshiri, F., Jensen, P.K., Qi, Q., Venkatesh, T.V., Karunanandaa, B., Baszis, S.R., Norris, S.R., Savidge, B., Gruys, K.J., Last, R.L., 2006. The Arabidopsis vitamin E pathway gene5-1 mutant reveals a critical role for phytol kinase in seed tocopherol biosynthesis. Plant Cell 18, 212–224.
Vranová, E., Coman, D., Gruissem, W., 2012. Structure and dynamics of the isoprenoid pathway network. Mol. Plant 5, 318–333.
Vrebalov, J., Ruezinsky, D., Padmanabhan, V., White, R., Medrano, D., Drake, R., Schuch, W., Giovannoni, J.J., 2002. A MADS-box gene necessary for fruit ripening at the tomato ripening-inhibitor (*RIN*) locus. Science 296, 343–346.
Wasternack, C., Hause, B., 2013. Jasmonates: biosynthesis, perception, signal transduction and action in plant stress response, growth and development. An update to the 2007 review in Annals of Botany. Ann. Bot. 111, 1021–1058.
Wilkinson, J.Q., Lanahan, M.B., Yen, H.C., Giovannoni, J.J., Klee, H.J., 1995. An ethylene-inducible component of signal transduction encoded by never-ripe. Science 270, 1807–1809.
Zanfini, A., Corbini, G., Rosa, C.L., Dreassi, E., 2010. Antioxidant activity of tomato lipophilic extracts and interactions between carotenoids and α-tocopherols in synthetic mixtures. LWT Food Sci. Technol. 43, 67–72.
Zhang, B., Horvath, S., 2005. A general framework for weighted gene co-expression network analysis. Stat. Appl. Genet. Mol. Biol. 4 (Article17).
Zhang, W., Liu, T., Ren, G., Hörtensteiner, S., Zhou, Y., Cahoon, E.B., Zhang, C., 2014. Chlorophyll degradation: the tocopherol biosynthesis related phytol hydrolase in Arabidopsis seeds is still missing. Plant Physiol.. http://dx.doi.org/10.1104/pp.114.243709.
Zhu, Z., An, F., Feng, Y., Li, P., Xue, L., A, M., Jiang, Z., Kim, J.M., To, T.K., Li, W., Zhang, X., Yu, Q., Dong, Z., Chen, W.Q., Seki, M., Zhou, J.M., Guo, H., 2011. Derepression of ethylene-stabilized transcription factors (EIN3/EIL1) mediates jasmonate and ethylene signaling synergy in Arabidopsis. Proc. Natl. Acad. Sci. U.S.A. 108, 12539–12544.